Direct imaging of intrinsic molecular orbitals using two-dimensional, epitaxially-grown, nanostructured graphene for study of single molecule and interactions

H. T. Zhou, J. H. Mao, G. Li, Y. L. Wang, X. L. Feng et al.

Citation: Appl. Phys. Lett. **99**, 153101 (2011); doi: 10.1063/1.3646406
View online: http://dx.doi.org/10.1063/1.3646406
View Table of Contents: http://apl.aip.org/resource/1/APPLAB/v99/i15
Published by the American Institute of Physics.

Direct imaging of intrinsic molecular orbitals using two-dimensional, epitaxially-grown, nanostructured graphene for study of single molecule and interactions

H. T. Zhou,[1] J. H. Mao,[1] G. Li,[1] Y. L. Wang,[1] X. L. Feng,[2] S. X. Du,[1] K. Müllen,[2] and H.-J. Gao[1,a)]
[1]*Institute of Physics, Chinese Academy of Sciences, Beijing 100190, China*
[2]*Max Planck Institute for Polymer Research, Ackermannweg 10, D-55128 Mainz, Germany*

(Received 16 June 2011; accepted 7 July 2011; published online 10 October 2011)

Using epitaxially grown graphene on Ru(0001) as a buffer layer, the intrinsic molecular orbitals of perylene-3,4,9,10-tetracarboxylic dianhydride, pentacene, and C_{60} molecules were imaged by means of scanning tunneling microscope (STM). Combined with density functional theory calculations, our high resolution STM images of the molecules reveal that the graphene layer decouples the individual molecules electronically from the metallic substrate. Our results show that graphene-based moiré pattern can be used as a unique way to probe the intrinsic electronic structures of molecular adsorbates and their interactions. © *2011 American Institute of Physics*. [doi:10.1063/1.3646406]

Direct imaging of the intrinsic electronic structure at high resolution is of both fundamental and technological importance for investigating molecular interaction and mechanisms, for example, bonding information and the dynamics. In the past years, scanning tunneling microscope (STM) has been demonstrated to be powerful for probing the detailed electronic structures of molecules on solid surfaces.[1,2] In previous studies, metallic (Au, Ag, Ru)[1,3] or semiconducting (Si, Ge, GaAs)[4] materials are commonly used as substrates for molecular adsorption. However, the strong interactions between molecules and metallic or semiconducting surfaces sometimes significantly change the intrinsic electronic and geometric structures of the adsorbed molecules.[5] Lu and coworkers reported a C_{60} adsorption on Ru(0001), in which STM image of the C_{60} showed no detailed molecular orbitals due to the strong interaction between the C_{60} and the Ru.[6] In order to overcome this problem, much effort has been made by passivating substrates with various buffer layers, for instance, thin organic films,[7] NaCl,[2] and oxides.[8] The intrinsic molecular orbitals of pentacene were obtained on a NaCl film covered Cu(111) surface,[2] but several issues remain to be overcome. The surface of oxides is relatively inhomogeneous with small domain sizes and many defects,[9] resulting in many different adsorption configurations of adsorbates.[10] In addition, buffer layers of organic films and NaCl cannot tolerate exposure to high temperatures and water, respectively.

Recently, graphene monolayer epitaxially grown on various metal surfaces, for example, Ru(0001),[11] Ir(0001),[12] Pt(111),[13] Ni(111),[14] and Cu(111),[15] have all attracted great interest due to their unique properties and potential applications for functional devices. Also, due to the ascending passions on graphene based organic devices, much effort on the growth of organic molecules on graphene has also been paid.[16,17] For instance, Barja and coworkers investigated the self-organizations of 7,7′,8,8′-tetracyano-p-quinodimethane (TCNQ) and 2,3,5,6-tetrafluoro-7,7,8,8-tetracyano-p-quinodimethane (F_4-TCNQ) on graphene grown on Ir(111) and found the two molecules adopted distinct molecular orderings.[16]

In this letter, we demonstrate that a large scale (centimeter), highly ordered, epitaxially grown graphene on Ru(0001) can be used as a buffer layer for direct imaging of the intrinsic electronic structures of the adsorbed molecules. Combining STM experiments with density functional theory (DFT) calculations, perylene-3,4,9,10-tetracarboxylic dianhydride(PTCDA), pentacene, and the fullerene (C_{60}) molecules are investigated. We found that the graphene layer allows high resolution imaging of the detailed molecular orbitals of adsorbed molecules by decoupling the molecules electronically from the Ru(0001) substrate.

The experiments were performed using a commercial Omicron low temperature STM system with a base pressure better than 1×10^{-10} mbar. The Ru(0001) surface was cleaned by cycles of argon-ion sputtering and annealing. High quality graphene was prepared by thermal decomposition of ethylene on this surface at high temperature. PTCDA, pentacene, C_{60} (Sigma, 99+%) molecules were thermally evaporated onto graphene at 620 K, 450 K, 600 K, respectively. During the evaporation processes, the substrates were kept at 300 K for PTCDA and C_{60} and 330 K for pentacene.

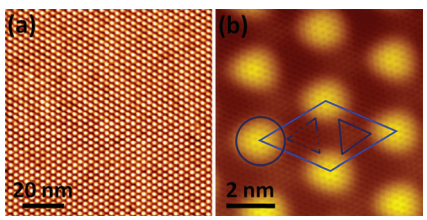

FIG. 1. (Color) STM images of graphene on Ru(0001). (a) Large-area image, showing regular moiré pattern. (b) Zoom-in image, showing the atomic resolution. A rhombus is overlaid to indicate the unit cell of moiré pattern. A circle, solid triangle, and dashed triangle are used to indicate the atop, fcc, and hcp regions, respectively. Scanning parameters: (a) $V_s = -3.0$ V, $I_t = 0.05$ nA and (b) $V_s = -0.2$ V, $I_t = 0.5$ nA.

a)Electronic mail: hjgao@iphy.ac.cn.

Subsequently, the samples were cooled down to 5 K for STM imaging. DFT calculations in this work were carried out using Gaussian03 code.

As shown in Fig. 1(a), graphene on Ru(0001) formed regular moiré pattern, remaining continuous and defect-free within the large scanned area. This pattern is induced by a lattice mismatch between Ru(0001) and graphene, with a periodicity of about 30 Å and an apparent corrugation of about 1 Å. Figure 1(b) is a zoom-in image with atomic resolution upon which a rhombus is superimposed to indicate the unit cell of the moiré superstructure. Three regions can be clearly distinguished in this unit cell: the bright region (marked by a circle), the less bright region (marked by a solid triangle), and the dark region (marked by a dashed triangle), which are assigned to the atop site, fcc site, and hcp site, respectively. We found that both the moiré pattern and high quality (defect-free) of the sample were preserved after the sample was annealed repeatedly at temperatures as high as 1300 K.

PTCDA, pentacene, and C_{60} molecules have been widely employed in understanding the mechanisms of molecular self-organization[17,18] and in electronic devices such as organic photovoltaic cells.[19,20] After the deposition of molecules on the graphene surface, we noted that PTCDA molecules self-assembled into a herringbone pattern on the graphene/Ru(0001) (Fig. 2(a)). A rectangle and molecular models are overlaid to indicate a unit cell of this pattern. In addition, another regular pattern appearing as six-fold symmetric bright spots can be clearly seen, whose unit cell is outlined by a rhombus in Fig. 2(a). This pattern is due to the superimposition of underlying moiré superstructures on PTCDA films, and an analogous phenomenon has also been observed for molecular film on reconstructed Au (111) surface, on which the reconstructed structure of Au(111) substrate can be seen after molecular deposition.[21] The PTCDA molecules normally show a herringbone arrangement on various low index noble metal surfaces, such as Au (111),[22] Ag (111),[22] and Cu (111).[23] However, interactions between molecules and these surfaces, including bonding, image charges, and metal-mediated lateral interaction,[24] give rise to a slight deformation of the herringbone unit cell compared to that of (102) plane of PTCDA bulk structure.[18] In the inset of Fig. 2(a), we measure the lattice parameters of the unit cell for PTCDA on graphene/Ru(0001), corresponding to $a_1 = 1.24$ nm, $a_2 = 1.93$ nm, and $\gamma = 90°$. Within the error limit, these three values are almost the same to those of β-phase (102) plane of PTCDA bulk structure, where $a_1 = 1.245$ nm, $a_2 = 1.930$, and nm, $\gamma = 90°$.[18,25] In addition, PTCDA molecules were completely desorbed when we annealed the sample to 360 K. Nevertheless, for molecules on metallic surfaces, higher desorption temperatures were needed and always accompanied by molecular dissociation.[18,26] These phenomena unambiguously indicate that the interactions between PTCDA and graphene/Ru(0001) are rather weak and inter-molecular interactions play a dominant role in the self-organization process.

In the zoom-in images of Fig. 2(b), the left and central images show the highest occupied molecular orbital (HOMO) and the lowest unoccupied molecular orbital (LUMO) of PTCDA molecules, respectively. The bias voltage in our STM system is the voltage of the sample with respect to that of tip, and thus negative and positive voltages correspond to HOMO and LUMO, respectively. These STM topographies fit very well with the calculated orbitals of a free molecule (as shown in the insets of Fig. 2(b)), which

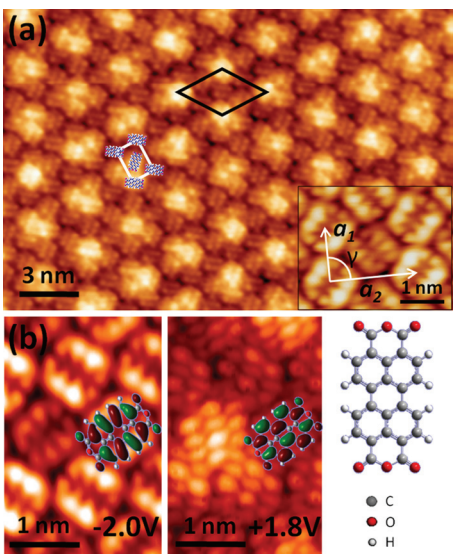

FIG. 2. (Color) STM images of PTCDA molecules adsorbed on graphene/Ru(0001). (a) Overview STM image, showing herringbone pattern. A rectangle and a rhombus are used to indicate the unit cells of the herringbone and moiré patterns, respectively. Inset displays a magnified unit cell with a_1 and a_2 denoting short and long lattice vectors. (b) High resolution images, showing HOMO (left panel) and LUMO (middle panel) with calculated orbitals superimposed. The right panel shows the molecular structure of PTCDA. Scanning parameters: (a) $V_s = -2.5$ V, $I_t = 0.05$ nA and (b) left: $V_s = -2.0$ V, $I_t = 0.1$ nA; middle: $V_s = 1.8$ V, $I_t = 0.2$ nA.

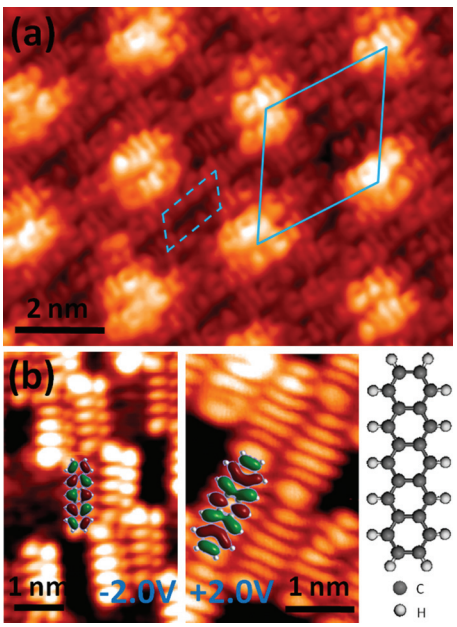

FIG. 3. (Color) STM images of pentacene molecules adsorbed on graphene. (a) Overview image, showing compact side-by-side rows. A dashed parallelogram and a rhombus are overlaid to outline the unit cells of molecular film and moiré pattern, respectively. (b) High resolution images, showing HOMO (left panel) and LUMO (middle panel) with calculated orbitals superimposed. The right panel shows the molecular structure of pentacene. Scanning parameters: (a) $V_s = 2.0$ V, $I_t = 0.05$ nA and (b) left: $V_s = -2.0$ V, $I_t = 0.05$ nA; middle: $V_s = 2.0$ V, $I_t = 0.05$ nA.

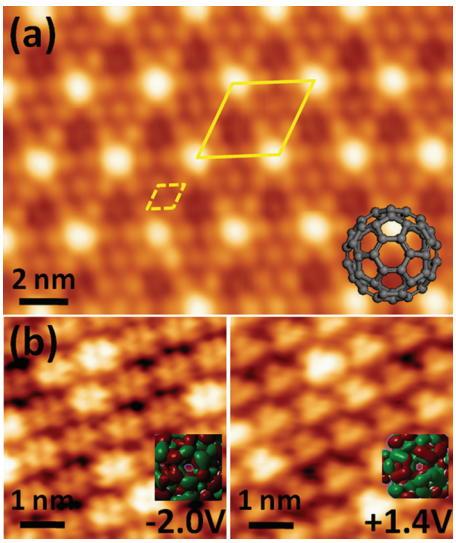

FIG. 4. (Color) STM images of C_{60} molecules adsorbed on graphene. (a) Overview image, showing close-packed pattern. A dashed rhombus and a solid rhombus are overlaid to outline the unit cells of molecular film and moiré pattern, respectively. Inset shows the molecular structure with a hexagon facing up. (b) High resolution images, showing HOMO (left panel) and LUMO (right panel). The insets show the calculated results. Scanning parameters: (a) $V_s = 2.0$ V, $I_t = 0.05$ nA and (b) left: $V_s = -2.0$ V, $I_t = 0.1$ nA; right: $V_s = 1.4$ V, $I_t = 0.1$ nA.

further verifies that the substrate exerts a weak influence and the intrinsic molecular orbitals are well preserved.

Pentacene and C_{60} molecules formed compact rows side-by-side and close-packed patterns, respectively, as shown in Figs. 3(a) and 4(a). Similar to the case of PTCDA, the unit cells of both molecular films and moiré patterns are outlined in the images. For pentacene, as presented in Fig. 3(b), the topographies agree well with the calculated results as shown in the insets. For C_{60}, the HOMO and LUMO images are in doughnut and three-leaf shapes, respectively (see Fig. 4(b)). Previous calculations suggest that the HOMO state is spatially located on C=C (double) bonds and the LUMO state on C–C (single) bonds.[27,28] Also, it is known that every bond shared by two adjacent hexagonal rings is an essential double-bond, while that on pentagonal rings is a single-bond in C_{60}. When we probe a C_{60} molecule with a hexagonal ring facing up (as shown in the inset of Fig. 4(a)), at negative bias (corresponding to HOMO), the double-bonded hexagonal rings are mainly detected, showing a doughnut image (left panel of Fig. 4(b)). While at positive bias (corresponding to LUMO), the single-bonded pentagonal rings are mainly detected, showing a three-leaf image (right panel of Fig. 4(b)).[28] Our topographies agree well with the above analysis and calculation results (see the insets of Fig. 4(b)). Thereby, based on these high resolution images, we can safely conclude that all the C_{60} molecules in the images adopt the same adsorption configuration with a hexagonal ring at the topmost position.

In conclusion, we have imaged the intrinsic molecular orbitals of three kinds of typical molecules (PTCDA, pentacene, and C_{60}) using epitaxially grown graphene on Ru(0001) as a buffer layer. The mechanism is due to the fact that the graphene disentangles the molecular electronic structure from the influence of the metallic substrate. Our results show that the graphene-based moiré pattern allows the high resolution STM imaging of the electronic structures of the adsorbed molecules. Moreover, it is in a large scale (centimeter in size), almost defect-free. Importantly, it is tolerant of high temperature (~1300 K) and water. Thus, it has a great potential application in the field of molecular science in directly detecting the molecular reaction mechanisms.

This work was financially supported by the NSFC (Nos. 10834011, 60976089) and MOST (Nos. 2009CB929103, 2010CB923004, and 2011CB932700) of China.

[1]H. J. Lee and W. Ho, Science **286**, 1719 (1999).
[2]J. Repp, G. Meyer, S. M. Stojkovic, A. Gourdon, and C. Joachim, Phys. Rev. Lett. **94**, 026803 (2005).
[3]F. Moresco, G. Meyer, K. H. Rieder, H. Tang, A. Gourdon, and C. Joachim, Appl. Phys. Lett. **78**, 306 (2001).
[4]Y. E. Cho, J. Y. Maeng, S. Kim, and S. Y. Hong, J. Am. Chem. Soc. **125**, 7514 (2003).
[5]T. C. Tseng, C. Urban, Y. Wang, R. Otero, S. L. Tait, M. Alcami, D. Écija, M. Trelka, J. M. Gallego, N. Lin, M. Konuma, U. Starke, A. Nefedov, A. Langner, C. Wolf, M. A. Herranz, F. Martín, N. Martín, K. Kern, and R. Miranda, Nat. Chem. **2**, 374 (2010).
[6]J. Lu, P. S. E. Yeo, C. K. Gan, P. Wu, and K. P. Loh, Nat. Nanotechnol. **6**, 247 (2011).
[7]Z. H. Cheng, S. X. Du, N. Jiang, Y. Y. Zhang, W. Guo, W. A. Hofer, and H.-J. Gao, Surf. Sci. **605**, 415 (2010).
[8]X. H. Qiu, G. V. Nazin, and W. Ho, Science **299**, 542 (2003).
[9]A. Stierle, F. Renner, R. Streitel, H. Dosch, W. Drube, and B. C. Cowie, Science **303**, 1652 (2004).
[10]S. W. Wu, N. Ogawa, and W. Ho, Science **312**, 1362 (2006).
[11]Y. Pan, H. G. Zhang, D. X. Shi, J. T. Sun, S. X. Du, F. Liu, and H. J. Gao, Adv. Mater. **21**, 2777 (2009).
[12]A. T. N'Diaye, S. Bleikamp, P. J. Feibelman, and T. Michely, Phys. Rev. Lett. **97**, 215501 (2006).
[13]H. Ueta, M. Saida, C. Nakai, Y. Yamada, M. Sasaki, and S. Yamamoto, Surf. Sci. **560**, 183 (2004).
[14]Y. S. Dedkov, M. Fonin, U. Rudiger, and C. Laubschat, Phys. Rev. Lett. **100**, 107602 (2008).
[15]X. S. Li, W. W. Cai, J. H. An, S. Kim, J. Nah, D. Yang, R. Piner, A. Velamakanni, I. Jung, E. Tutuc, S. K. Banerjee, L. Colombo, and R. S. Ruoff, Science **324**, 1312 (2009).
[16]S. Barja, M. Garnica, J. J. Hinarejos, A. L. V. de Parga, N. Martin, and R. Miranda, Chem. Commun. **46**, 8198 (2010).
[17]Q. H. Wang and M. C. Hersam, Nat. Chem. **1**, 206 (2009).
[18]F. S. Tautz, Prog. Surf. Sci. **82**, 479 (2007).
[19]N. S. Sariciftci, D. Braun, C. Zhang, V. I. Srdanov, A. J. Heeger, G. Stucky, and F. Wudl, Appl. Phys. Lett. **62**, 585 (1993).
[20]P. Peumans and S. R. Forrest, Appl. Phys. Lett. **79**, 126 (2001).
[21]H.-J. Gao and L. Gao, Prog. Surf. Sci. **85**, 28 (2010).
[22]S. K. M. Henze, O. Bauer, T. L. Lee, M. Sokolowski, and F. S. Tautz, Surf. Sci. **601**, 1566 (2007).
[23]T. Wagner, A. Bannani, C. Bobisch, H. Karacuban, and R. Moller, J. Phys.: Condens. Matter **19**, 056009 (2007).
[24]A. Hauschild, K. Karki, B. C. C. Cowie, M. Rohlfing, F. S. Tautz, and M. Sokolowski, Phys. Rev. Lett. **94**, 036106 (2005).
[25]K. Glockler, C. Seidel, A. Soukopp, M. Sokolowski, E. Umbach, M. Bohringer, R. Berndt, and W. D. Schneider, Surf. Sci. **405**, 1 (1998).
[26]P. Fenter, F. Schreiber, L. Zhou, P. Eisenberger, and S. R. Forrest, Phys. Rev. B **56**, 3046 (1997).
[27]L. L. Wang and H. P. Cheng, Phys. Rev. B **69**, 165417 (2004).
[28]Y. Maruyama, K. Ohno, and Y. Kawazoe, Phys. Rev. B **52**, 2070 (1995).